

Research Article

Study on Double Pressure Funnels and Gas-Liquid Two-Way Mass Transfer after Fracturing in Shale Gas Reservoirs

Zhiwei Lu^{1,2}, Xizhe Li^{1,2,3}, Xing Liang⁴ and Youzhi Hao⁵

¹School of Engineering Science, University of Chinese Academy of Sciences, Beijing 100049, China

²Institute of Porous Flow and Fluid Mechanics, Chinese Academy of Sciences, Langfang 065007, China

³Research Institute of Petroleum Exploration and Development, PetroChina, Beijing 100083, China

⁴PetroChina Zhejiang Oilfield Company, Hangzhou 310023, China

⁵Department of Modern Mechanics, University of Science and Technology of China, Hefei 230027, China

Correspondence should be addressed to Xizhe Li; lxz69@petrochina.com.cn

Received 27 September 2022; Revised 21 November 2022; Accepted 22 November 2022; Published 13 December 2022

Academic Editor: Shengnan Nancy Chen

Copyright © 2022 Zhiwei Lu et al. This is an open access article distributed under the Creative Commons Attribution License, which permits unrestricted use, distribution, and reproduction in any medium, provided the original work is properly cited.

Well shut-in and drainage after shale gas fracturing are important factors affecting the productivity. Due to the imperfect optimization method of shale gas flowback, there has been no clear explanation for the problems such as “formulation of reasonable well shut-in time” and “less fracturing fluid flowback but high-gas production phenomenon” during shale gas drainage. In this paper, the double pressure funnels (one funnel is formed during fracturing by pressure difference from wellbore to formation, and two funnels are formed during flowback by pressure difference from fracture to formation and from fracture to wellbore) and gas-liquid two-way mass transfer (gas transfer by diffusion and liquid transfer by pressure difference) in shale gas drainage are investigated by calculating the pressure distribution after fracturing shale gas wells. The discrete numerical simulation by using unstructured PEBI grid is conducted, and the result is as follows: when shale gas well is shut-in for 20 days and produce for 1 year, the daily gas production corresponding to fracturing fluid flowback rates of 20%, 10%, and 5% are 47700 m³, 5800 m³, and 72700 m³, respectively. The investigation of double pressure funnels and gas-liquid two-way mass transfer explains clearly the phenomenon “less fracturing fluid flowback but high-gas production.” Meanwhile, the two conditions for optimizing the well shut-in time after fracturing are presented. That is, as for the studied case, the moving speed of the pressure boundary line should be less than 0.1 m/d, and the water-gas ratio near the fracture should be less than 1/d with time. Consequently, the reasonable well shut-in time is optimized to be 20–25 days. The findings in this work are of benefit to enrich the flowback theory of shale gas after fracturing and provide a theoretical basis for the optimization technology of shale gas drainage after fracturing.

1. Introduction

With the rapid development of horizontal well drilling and multistage fracturing technology, unconventional natural gas has been effectively developed on a large scale [1, 2]. Sichuan Basin is the main shale gas producing area in China and one of the fastest growing shale gas production areas in the world [3, 4]. Since 2010, high-production shale gas resources have been found in Changning-Weiyuan, Zhao-tong, Fuling, and other blocks, and three marine shale gas industrial-demonstration areas have been established [5]. In the long-term practice of shale gas development, unusual

phenomena such as “the lower the flowback of the gas well, the higher the production after fracturing,” and “when the gas well is opened after shut-in for a period, the gas production increases but the liquid production decreases” [6] have been found. Also, the development system such as well shut-in after fracturing and small nozzle gas testing are preliminarily formed. Researchers up to now have carried out many experiments and numerical simulation studies in shale gas development [7–11], but they have not obtained a systematic understanding to explain the unusual phenomena found in engineering practices, nor have they quantitatively given the well shut-in time and drainage system.

Shale gas development generally goes through fracturing, well shut-in, and flowback stages before production stage. The essence of internal changes in shale reservoirs during these different stages is the redistribution of pressure and the transfer of liquid and gas. At present, researches on shale gas fracturing, well shut-in, and drainage mainly focus on three aspects: flow mechanism, complex fracture network formed by multistage fracturing of horizontal wells, and simulation and optimization during drainage stages.

Shale gas seepage mechanism covers the range of molecular scale, micro and nanopores, and macroscale [12], and there are migration modes such as slip, adsorption, diffusion, and seepage [13, 14]. The purpose of the study on shale gas seepage mechanism is to provide mathematical models for the development of shale gas at various stages of gas fracturing, well shut-in, and drainage. The most important one is modified Darcy's law. For example, the modified apparent permeability can describe the slippage, pressure-sensitive, and diffusion effects of shale gas that deviate from the traditional cognition [15–17].

The network structure and area generated after fracturing determine the flow boundary range of gas-liquid two-phase flow in well shut-in and drainage. Since it is impossible to directly measure the fracture-network type and SRV area after fracturing, it is important to use fracture propagation model for simulation and calculation. Common fracture propagation simulation includes two-dimensional, quasi three-dimensional, plane three-dimensional, and full three-dimensional models [18, 19]. The most practical and reliable model for shale gas multistages fracturing is the plane three-dimensional model [20, 21]. Another method to obtain the fracture morphology and SRV area after fracturing is the fracturing construction-data inversion [22]. By establishing the wellhead-pressure-drop curve chart after the hydraulic-fracturing stop-pump, the parameters such as fracture network morphology, fracture half-length, and SRV area permeability can be obtained through curve fitting.

The researches of shale gas well shut-in and drainage optimization are mainly experiments and numerical simulations. Yu et al. [23] applied nonintrusive EDFM (embedded-discrete fracture model) to couple fracture and reservoir models, and numerical simulation with and without considering nature fractures is conducted in shale gas development. As shown in complex fracture (considering nature fractures) system, it has large drainage area and high-drainage efficiency, therefore the cumulative gas and water production will be larger than simple fractures (without considering nature fractures) system. Chen et al. [24] used the structured grid near the fracture to simulate the unified flowback of multilayer fracturing; Eltahan et al. [25] conducted 3D-reservoir simulation of complex fractured network that intermeshes with formation matrix and studied well shut-in impact on the productivity and recovery of shale oil reservoirs; Wijaya and Sheng [26] conducted a flow-geomechanical model to study the relationship between imbibition and well shut-in; it shows only if imbibition dominated during recovery in shale reservoir, well shut-in tends to improve both the ultimate oil recovery and net present value (NPV); Tao et al. [27] designed a water spontaneous imbibition apparatus, though

clay mineral content measurement and salt ion concentration diffusion experiment, the optimal shut-in time for type I and type II shale reservoir are 20 days and 15 days, respectively. Wu et al. [28] proposed a two-phase flow model considering formation damage caused by clay expansion and gave a semianalytical-solution model based on Laplace transform, but this method is mainly used for production data analysis and prediction of tight gas wells.

The three aspects involved in the study of shale gas fracturing, well shut-in and drainage in the existing literature are independent of each other. The numerical simulation of well shut-in and drainage bases on the assumption of constant initial pressure and use structured grid finite difference. It is obvious that the structured grids are difficult to characterize the complex fracture network of horizontal well multistage fracturing, especially during fracturing, a large amount of fracturing fluid enters the formation, and the pressure near the wellbore is several times of the original formation pressure, so the assumption that the initial pressure keeps constant is unreasonable. At the same time, the existing simulation results can only analyze the impact of some parameters on well shut-in and drainage and have not summarized reasonable rules and effective optimization methods from the simulation results.

In this paper, the unstructured PEBI grid is used to replace the structured grid, and the finite volume method is used to discrete shale gas-water two-phase equation to realize the accurate characterization of the fracture. The pressure distribution after fracturing is obtained by using the multidimensional instantaneous source function as the initial pressure condition for well shut-in and drainage simulation, so the gas-liquid two-phase simulation of shale is carried out. According to the simulation results, the understanding of “double pressure drop funnels” and “gas-liquid two-way mass transfer” is proposed, and some phenomena in the process of shale gas development are well explained. Meantime, it also provides a theoretical basis for the optimization of drainage system in shale gas production.

2. Theory and Optimization Method

Large scale fracturing of shale gas results in a large amount of fracturing fluid entering the formation. During fracturing stage, high pressure near the fracture gradually spreads to the far distance from formation with low formation pressure, and a large reversed pressure difference is formed (defined as reversed pressure funnel). Also during the drainage stage after fracturing, the high-pressure area near the fracture and the low-pressure area near the wellbore also form a pressure funnel due to pressure difference, resulting in the phenomenon of double-pressure funnels, and the liquid follows the seepage law from high to low pressure and migrates to the far distance from formation. On the other hand, the area near the fracture is occupied by large amount of fracturing fluid, so the gas concentration is close to 0, while the far distance from formation is not affected by the fracturing fluid so the gas concentration is close to 100%. Due to the concentration difference, the gas diffuses from the far distance from formation to the vicinity of the

fracture, causing the phenomenon of gas-liquid two-way mass transfer. The mechanism of double pressure funnels and gas-liquid two-way mass transfer are special phenomena in shale gas development (Figures 1 and 2).

2.1. Pressure Distribution Caused by Fracturing Fluid Injection. There is a vertical-fractured well in the closed-rectangular formation, and the well location and boundary are shown in Figure 3. We assume that there is a fracture

$$p(x, y, t) = p_i + \frac{G}{\phi\mu C_t y_e} \left\{ 1 + 2 \sum_{n=1}^{\infty} e^{-(3.6n^2\pi^2\chi t/y_e^2)} \cos\left(\frac{n\pi y_w}{y_e}\right) \cos\left(\frac{n\pi y}{y_e}\right) \right\} \cdot \frac{x_f}{x_e} \left\{ 1 + \frac{2x_e}{\pi x_f} \sum_{n=1}^{\infty} \frac{1}{n} e^{-(3.6n^2\pi^2\chi t/x_e^2)} \sin\left(\frac{n\pi x_f}{x_e}\right) \cos\left(\frac{n\pi x_w}{x_e}\right) \cos\left(\frac{n\pi x}{x_e}\right) \right\}, \quad (1)$$

where $\chi = k/(\phi\mu C_t)$ is pressure coefficient, (m^2/s); k is formation permeability (μm^2); ϕ is the formation porosity; h is the effective thickness of the formation, (m); μ is the fluid viscosity in the formation, ($\text{MPa}\cdot\text{s}$); C_t is the comprehensive compression coefficient, (MPa^{-1}); p_i is the original formation pressure, (MPa); x_f is the half-length of the fracture, (m); G is the total amount of injected fracturing fluid, (m^3); (x_w, y_w) is the well location, (m); (x_e, y_e) is the side length of the rectangular boundary, (m).

2.2. Mathematical Model of Gas-Liquid Two-Phase Flow with PEBI Grid. After the multistage fracturing of horizontal wells forms a complex fracture network, the shale is divided into two systems: bedrock and fracture. The shale desorption only occurs in the bedrock when formation pressure is low. The desorbed gas enters the fracture network from the bedrock through diffusion, and the adsorption effect can be ignored. Considering that shale gas is mainly natural gas dominated by methane, the black oil model can be used for gas-liquid two-phase seepage. Meanwhile, the PEBI grid can accurately characterize the internal boundaries of wells and fractures in the multistage fracturing of horizontal wells. The PEBI grid is an unstructured grid [31], each grid is adjacent to multiple grids, and the number of adjacent grids is not fixed. As shown in Figure 4, there are 6 grids numbered 0-5 around the grid i . Due to the orthogonality of PEBI grid, finite volume method is used to discretize the shale gas-liquid two-phase process.

Consider any grid i in the PEBI grid shown in Figure 5. Assuming the grid that adjacent to the grid i is j , and $\sum j_{\text{sign}}$ represents the summation of all adjacent grids of grid i , the implicit discrete equations of water and gas phase equations are

$$\sum_j [T_{ij,w}(\Delta p - \gamma_w \Delta Z)]^{n+1} = C_{wp} \delta p + C_{ww} \delta S_w, \quad (2)$$

in the rectangular area, the fluid in the formation is slightly compressible, and the half-length of the fracture is x_f .

Compared with the pressure buildup test after shale gas production for a long time, the injection time of fracturing fluid during fracturing construction is shorter. Therefore, the fracture liquid is assumed to be injected instantaneously ($\tau = 0$). The pressure distribution of the vertical-fracture well can be derived by using the instantaneous source function [29] and Newman product method [30]. That is,

$$\sum_j \left[(T_{ij,g} + D_m C_g) (\Delta p - \gamma_g \Delta Z) \right]^{n+1} = C_{gp} \delta p + C_{gg} \delta S_g, \quad (3)$$

where $T_{ij,l} = \lambda_{ij,l} G_{ij}$ is the conductivity coefficient ($\text{m}^3/\text{Pa}\cdot\text{s}$), and the geometric factor G_{ij} is the ratio of the area ω_{ij} (the adjacent surface of two adjacent grids i and j) multiply permeability K_{ij} to the distance between the center points of these two grids d_{ij} [32]. That is

$$G_{ij} = \frac{k_{ij} \omega_{ij}}{d_{ij}}, \quad (4)$$

wherein $\lambda_{ij,l}$ is the ratio of relative permeability to the viscosity and volume coefficient

$$\lambda_{ij,l} = \left(\frac{k_{rl}}{\mu_l B_l} \right)_{ij}. \quad (5)$$

Other variables in Equations (2) and (3) are defined as follows:

$$C_{wp} = \frac{V_i}{\Delta t} \left[\frac{1}{B_w^n} \frac{\partial \phi}{\partial p} + \phi^{n+1} \frac{\partial (1/B_w)}{\partial p} \right] S_w^n \quad (6)$$

$$C_{ww} = \frac{V_i}{\Delta t} \left(\frac{\phi}{B_w} \right)^{n+1} \quad (7)$$

$$\Delta p = p_j - p_i \quad (8)$$

$$\Delta Z = Z_j - Z_i \quad (9)$$

$$\delta f = f^{n+1} - f^n \quad (10)$$

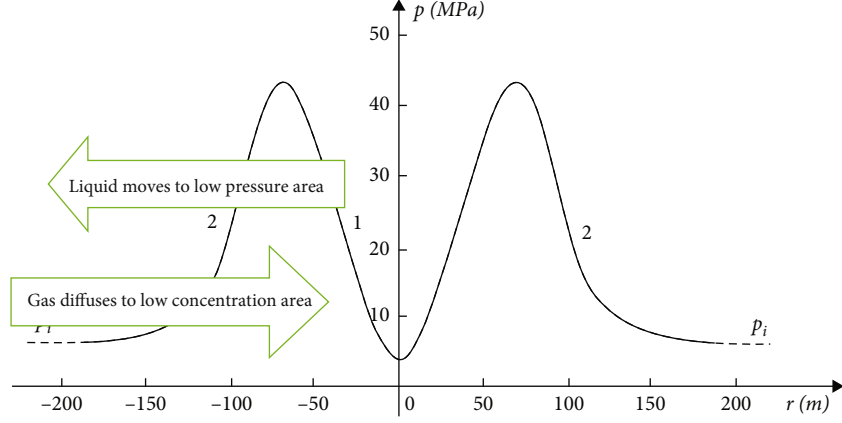


FIGURE 1: Schematic diagram of double pressure funnels and gas-liquid two-way transfer theory.

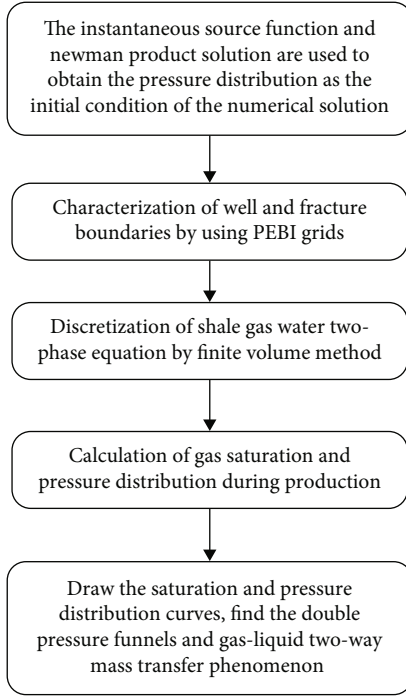


FIGURE 2: Flowchart of work steps.

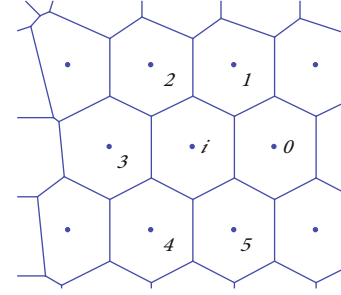


FIGURE 4: PEBI grid i and its adjacent grids, with adjacent grids numbered 0-5.

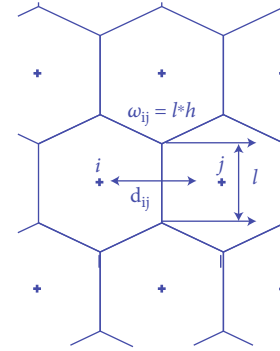


FIGURE 5: Parameters between grids i and j .

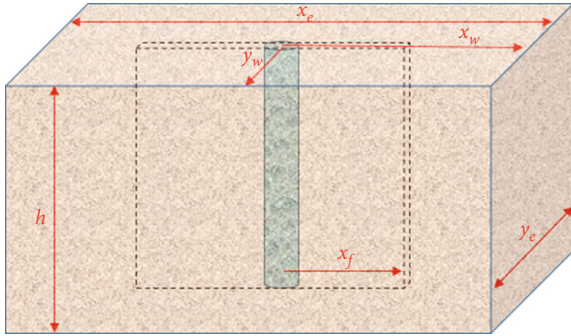


FIGURE 3: Model of a vertical-fractured well in rectangular-closed formation.

$$C_{gp} = \frac{V_i}{\Delta t} \left[\frac{1}{B_g^n} \frac{\partial \phi}{\partial p} + \phi^{n+1} \frac{\partial (1/B_g)}{\partial p} \right] S_g^n \quad (11)$$

$$C_{gg} = \frac{V_i}{\Delta t} \left(\frac{\phi}{B_g} \right)^{n+1} \quad (12)$$

where Z is the height calculated from a certain datum (m); k_{rl} , μ_l , γ_l , and B_l ($l = w, g$) are the relative permeability, viscosity (Pa.s), underground fluid gravity, and volume coefficient of the l phase, respectively; f is the solution variables of p , S_w , and S_g ; ϕ is porosity; C_g is the gas compression coefficient, (Pa^{-1}); V_i is the volume of the i^{th} grid unit, (m^3); $\Delta t = t^{n+1} - t^n$ is the time step length difference

TABLE 1: Basic parameters of a shale gas well.

Parameter	Value
Formation original pressure (MPa)	38.73
Gas diffusion coefficient, (m ² /s)	2.2*10 ⁻⁷
Porosity	0.056
Formation thickness (s)	38
Well radius (m)	0.1
Number of fractures	20
Horizontal well length (m)	1000
Rectangle side length X (m)	2000
Total fracturing fluid (m ³)	26639.4
Formation temperature (°C)	118.65
Gas compressibility (MPa ⁻¹)	0.054
Matrix permeability (mD)	0.038
Fracturing fluid viscosity (MPa.s)	40
Compression coefficient (MPa ⁻¹)	0.000413
Average half-length of fractures (m)	70
Methane content (%)	100
Rectangle side length Y (m)	600
Sand addition (m ³)	1206

of $n + 1$ time step length and n time step length, (s); subscript w indicates water phase and subscript g indicates gas phase.

3. Calculation and Analysis

To demonstrate the utility of the proposed theory in this paper, a shale gas well is taken as an example. The parameters used in the calculation are given in Table 1 for 20 stages fractured-horizontal well in the center of the rectangular reservoir.

3.1. Double Pressure Funnels Phenomenon of Flowback after Fracturing. Large amount of fracturing fluid enters the formation during fracturing, and a high-pressure area is formed near the wellbore. When flowback after fracturing, on the one hand, a pressure funnel is formed between the high-pressure area of fracturing fluid near the fracture and the original formation pressure, on the other hand, a funnel is formed near the fracture where the fracturing fluid flows back, which results in double pressure funnels phenomenon. In order to calculate the double pressure funnels, the analytical solution is combined with the PEBI grid numerical simulation. The initial pressure distribution calculated by Equation (1) is used in the PEBI grid numerical simulation. Assume the flowback rate is 400 m³/d (the flowback rate of single fracture is 20 m³/d), Figure 6 shows the 5-day single fracture double pressure funnels diagram. Figure 7 is the pressure change curve of single fracture along the fracture direction in the formation. There are two kinds of flow phenomena when fracturing fluid flows back. One is flowing from fracture to the wellbore (corresponding to zone 1 in Figure 7), and the other is flowing from fracture to the far distance from formation (corresponding to zone 2 in

Figure 7). Zone 1 in Figure 7 is a pressure funnel area near the fracture when the fracturing fluid flows back to the wellbore, and zone 2 is another pressure funnel area formed by the high-pressure area caused by fracturing fluid near the fracture and the original formation pressure.

Figure 8 displays the formation pressure distribution of 20 fractures in 5 days after flowback. The red area (63.84 MPa) in Figure 8 is the high-pressure area caused by the injection of fracturing fluid between the two fractures, and the blue area (34.61 MPa, which is lower than the original formation pressure) is the pressure distribution near the fractures. Figure 9 illustrates the 3D pressure-distribution diagram of Figure 8. The double pressure funnels phenomenon can be found near each fracture during fracturing fluid flowback.

3.2. Gas-Liquid Two-Way Transfer Phenomenon after Fracturing. In multiphase system, the motivation of gas satisfies Fick's diffusion law. The velocity v_a caused by diffusion [28, 33] can be expressed as

$$\vec{V}_a = -\frac{D_m}{C} \nabla C, \quad (13)$$

where D_m is gas diffusion coefficient (m²/s), and $c = m/v$ is the gas concentration (kg/m³). From the definition of concentration, for the gas diffusion in the formation, the concentration means density of the gas in the formation. According to the equation of state of the real gas, the density of the gas can be expressed as [30, 34]

$$\rho = \frac{pM}{RzT}. \quad (14)$$

According to the definition of gas compression coefficient [30],

$$C_g = \frac{1}{\rho} \frac{dp}{dp}. \quad (15)$$

According to Equations (14) and (15), the velocity of gas migration V_a caused by diffusion can be rewritten as

$$\vec{v}_a = -D_m C_g \nabla p, \quad (16)$$

where M is the unit molar mass of the gas mixture (kg/kmol), $R = 8.314$ is the universal gas constant kg/(kmol.k), z is the deviation factor of real gas, and T , ρ , and c_g is the gas temperature (k), density (kg/m³), and compression coefficient (MPa⁻¹), respectively. By comparing the gas seepage equation, the gas migration velocity is the sum of the seepage velocity and the diffusion velocity. In this way, the gas phase conductivity coefficient $\lambda_{ij,g}$ from Equation (5) under the PEBI grid can be defined

$$\lambda_{ij,g} = \left(\frac{K_{rg}}{\mu_g B_g} + \frac{D_m c_g}{B_g} \right)_{ij}. \quad (17)$$

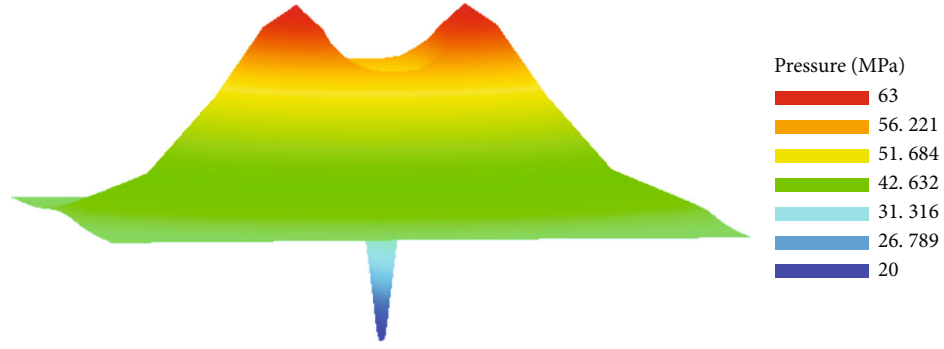


FIGURE 6: Double pressure funnels phenomenon of pressure distribution perpendicular to the fracture direction when a single fracture flows back for 5 days.

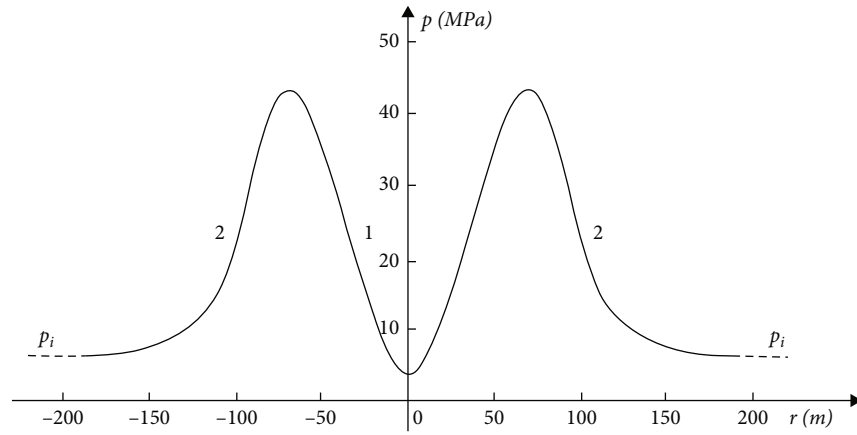


FIGURE 7: Pressure distribution perpendicular to fracture direction during single fracture fracturing fluid flowback.

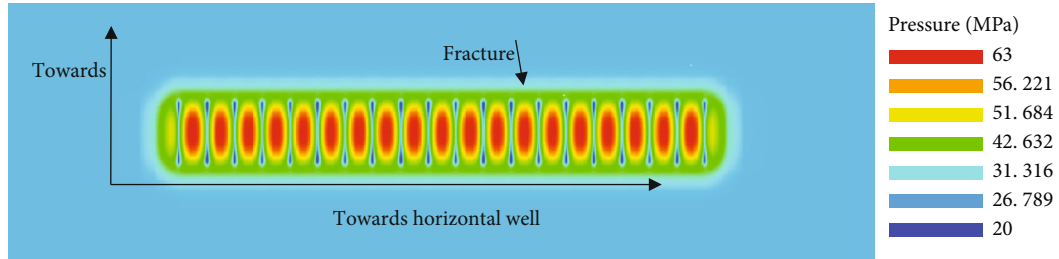


FIGURE 8: Isoline cloud figure of pressure distribution along fracture direction of fracturing fluid flows back for 5 days in a multistage fractured-horizontal well.

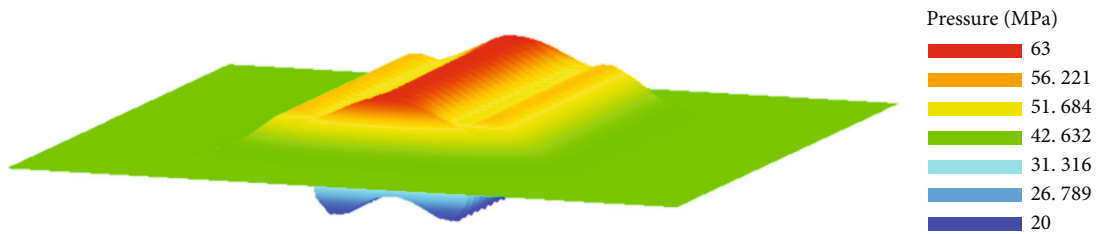


FIGURE 9: Formation pressure distribution of 5 days fracturing fluid flowback in multistage fracturing horizontal well.

Using the data in Table 1 and unstructured PEBI grid numerical simulation program, the diffusion of gas in fracturing fluid is calculated. Free gas content V_g in the for-

mation (m^3/T). Figure 10 shows the change of water-gas ratio near the fracture with well shut-in time under different free gas content of shale.

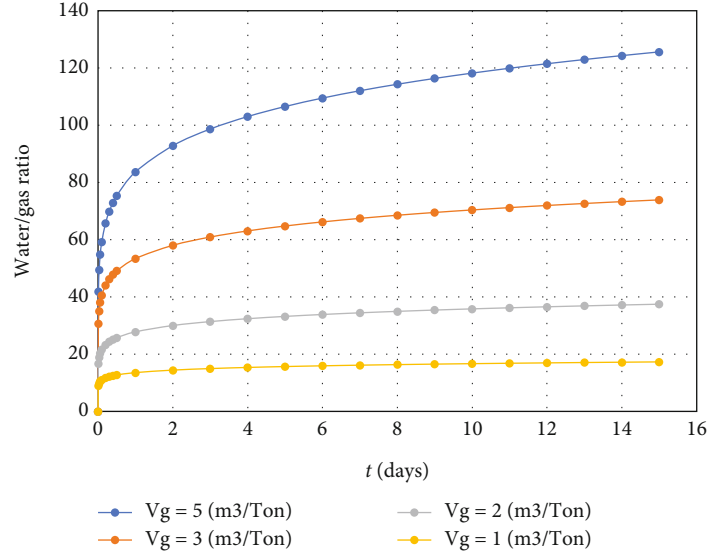


FIGURE 10: Water-gas ratio under different free gas contents in shale.

It can be seen from Figure 10 that during the stop-pump and well shut-in period, the gas content in the water near the fracture is zero when the pump is just stopped. With the increase of the shut-in time, the gas content in the water gradually increases, but the change rate of the gas content in the water decreases with the increase of time. When the shut-in time is long, the gas content in the water becomes a constant. It can also be seen in Figure 10 that the free gas content in the formation also affects the water-gas ratio. When V_g is small, the water-gas ratio curve near the fracture becomes constant in a short time. For example, if $V_g = 1$, the water-gas ratio curve approaches constant after 3 days shut-in. If $V_g = 5$, the water-gas ratio curve still rising after 15 days shut-in. At the same time, if V_g is large, the water-gas ratio near the fracture is large.

Figure 11 is the gas and water saturation distribution for 1 day well shut-in. Figure 12 is the gas and water saturation distribution for 5 days well shut-in. The red area represents $S_g = 1$, and the blue area represents $S_g = 0$. It can be seen with time increasing, gas accumulates near the wellbore. It shows that gas can move from high-pressure area to low-pressure area by diffusing.

4. Application

4.1. Theoretical Explanation for Low Flowback of Fracturing Fluid but High-Gas Production. If large amount of fracturing fluid flows back, it means the formation permeability is good. Because the viscosity of gas is far less than that of liquid, according to the conventional seepage theory, the gas production should be high. However, an unusual phenomenon which is “if less fracturing fluid flows back, the gas production will be high” exists in shale gas development. There have been no reasonable theoretical explanations. The proposed double pressure funnels and gas-liquid two-way transfer theory can well explain this phenomenon.

After fracturing of shale reservoir, a large reconstruction area is formed. After fracturing fluid enters the formation, a pressure imbalance area with high pressure near the wellbore and low pressure at far distance from formation is formed. The fracturing treatment effectively improves the permeability of the formation. The fracturing fluid flows to the far distance from formation through seepage, which is equivalent to increasing the average pressure of the formation. On the other hand, the initial concentration of gas in the fracturing fluid near the wellbore is almost zero, and the high-concentration gas in the fracturing reconstruction affected area enters the vicinity of the fracture through diffusion, resulting in the phenomenon of gas-liquid two-way mass transfer. When flowing back after fracturing, with the production of liquid and gas, the pressure near the wellbore decreases, and the pressure funnel in zone 1 in Figure 13 gradually advances to the far distance from formation. At the same time, the fracturing fluid in zone 2 also continues to advance to the far distance from formation, further improving the average formation pressure. If there is less flowback liquid, the double funnel phenomenon exists for a long time, the formation maintains high pressure for a long time, and the gas production is high. On the contrary, if there is more flowback fluid, the double funnel phenomenon will soon disappear; the formation is difficult to maintain high pressure, so the gas production will be less.

4.2. Determination of the Reasonable Shut-In Time. There are many qualitative descriptions of shale gas shut-in time but few quantitative calculation methods. The theory of double pressure funnels and gas-liquid two-way mass transfer in this paper can quantitatively give the reasonable well shut-in time. During the shut-in period of shale gas well after fracturing, due to the phenomenon of pressure funnel between the wellbore and the formation, the formation pressure redistributes with time. Figure 14 shows the pressure distribution under different well shut-in times calculated by the parameters in Table 1. The pressure near the wellbore

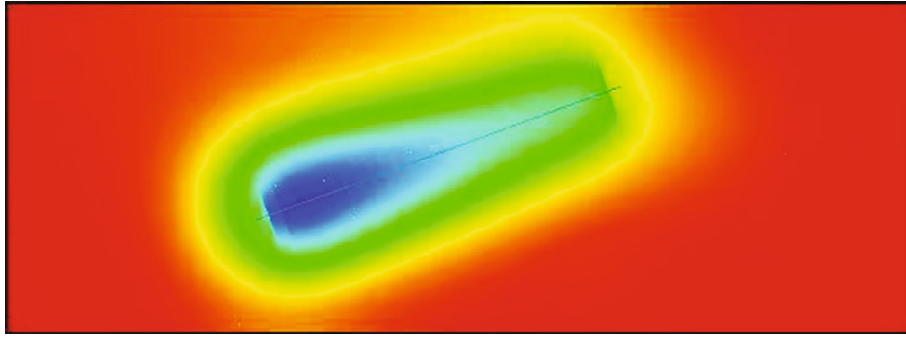


FIGURE 11: Gas saturation distribution of 1 day well shut-in.

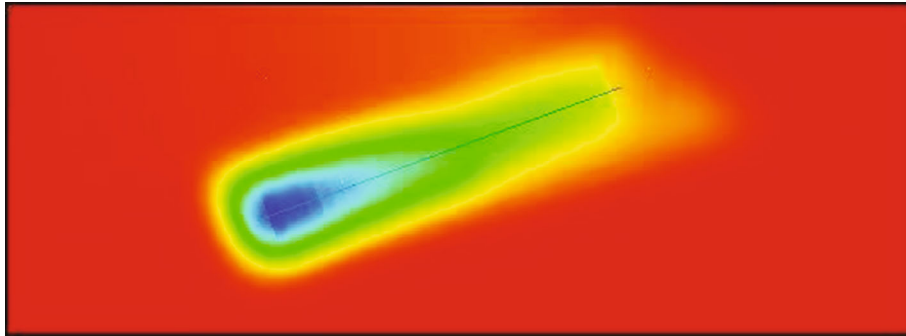


FIGURE 12: Saturation distribution of 5 days well shut-in.

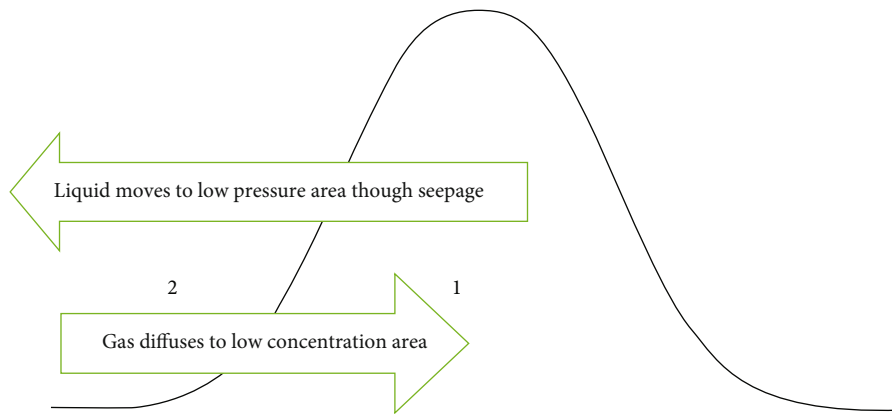


FIGURE 13: Schematic diagram of gas-liquid two-way transfer in fractured well.

flattens with the increase of time during the shut-in period, and the pressure also diffuses outward. The relative difference between the value of the pressure isoline and the original formation pressure equals to 0.1% is defined as the pressure boundary line. The pressure requirements of the well shut-in are determined by the moving speed of the pressure boundary line.

Free gas will diffuse due to concentration difference. When large amount of fracturing fluid enters near the wellbore, the concentration of gas in the fracturing fluid is zero. If the content of free gas in the formation is high, the gas will diffuse from the low-pressure area of the formation rich in free gas to the fracturing fluid in the high-pressure area due to concentration difference, and at the same time, a part

of the gas displaced by water will also diffuse to the fracturing fluid near the wellbore. When the shut-in time is long enough, the fracturing fluid and gas reach a new equilibrium. The time for gas diffusion reaches equilibrium varies with the content of free gas.

The moving speed of the pressure boundary line and the diffusion equilibrium time of free gas are the two conditions for determining the reasonable well shut-in time. Through calculation and combined with the field experience of shale gas development in Zhejiang oilfield of PetroChina and some other fields of Sinopec, the reasonable well shut-in time should meet the following requirements: the moving speed of the pressure boundary line is less than (0.1 m/d). The water-gas ratio change rate with time near the fracture

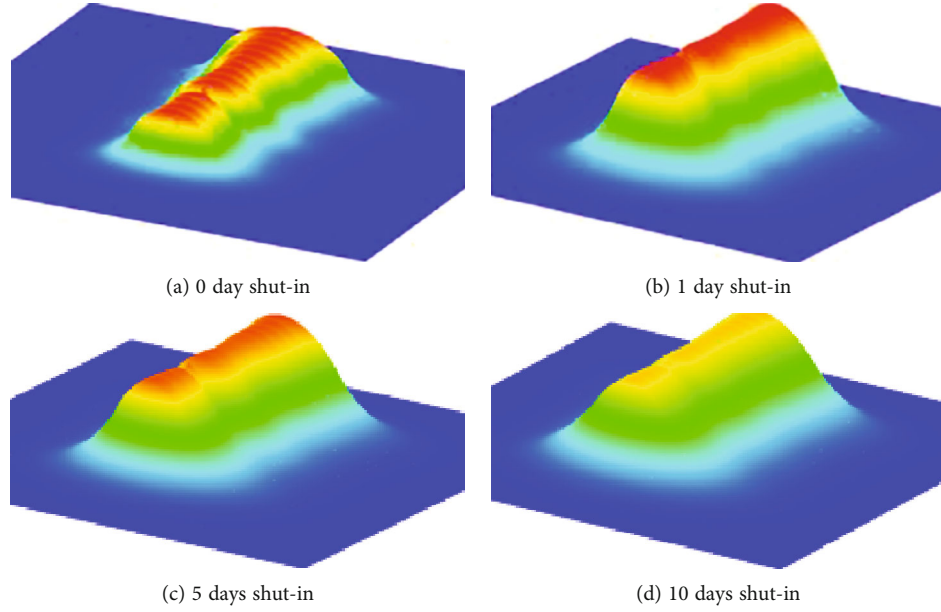


FIGURE 14: Formation pressure distribution for different well shut-in times.

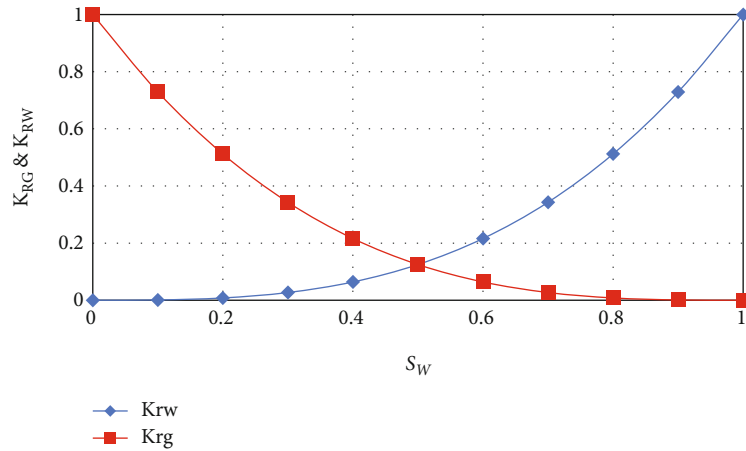


FIGURE 15: Gas-water two-phase relative permeability curves.

is less than $(1/d)$. When the above conditions are met, the top of the pressure near the wellhead flattens and the shape of the pressure funnel hardly changes. For shale gas wells, the roughly shut-in time is around 20-25 days (according to the fracturing scale).

In order to ensure the reliability of the calculation, a high-precision pressure gauge is installed at the wellhead during fracturing, with the sampling frequency of 1 Hz. The wellhead pressure is converted to the bottom-hole pressure using the wellbore two-phase flow program. The measured bottom-hole pressure must be consistent with the calculated bottom-hole pressure, ensuring the effectiveness of the algorithm.

4.3. Relationship between Shale Gas Flowback Rate and Gas Productivity. Shale gas drainage is water-gas two-phase seepage of complex fracture network [35] (including diffusion).

Figure 15 is the gas-water two-phase seepage curve used in the calculation, which is calculated by using the PEBI grid program. The initial pressure distribution in the numerical simulation is calculated by using Formula (1) from the data in Table 1. For 20 days well shut-in time and the free gas content $V_g = 5 \text{ (m}^3/\text{T)}$, according to the gas diffusion equation, the change of gas concentration during the well shut-in after pressure can be calculated. The calculation method provided here is also applicable to dual media. The main flow channel [36] can be used to equivalent the dual media to gas-water two-phase seepage in the fracture network.

Based on the above calculation, as shown in Figure 16, the production curve with time in one year is simulated when the flowback rate is 5%, 10%, and 20%, respectively. The results shown that: (1) at the initial stage of flowback, the maximum daily output of gas is 214000 m^3 , and the maximum daily output is less affected by the flowback rate

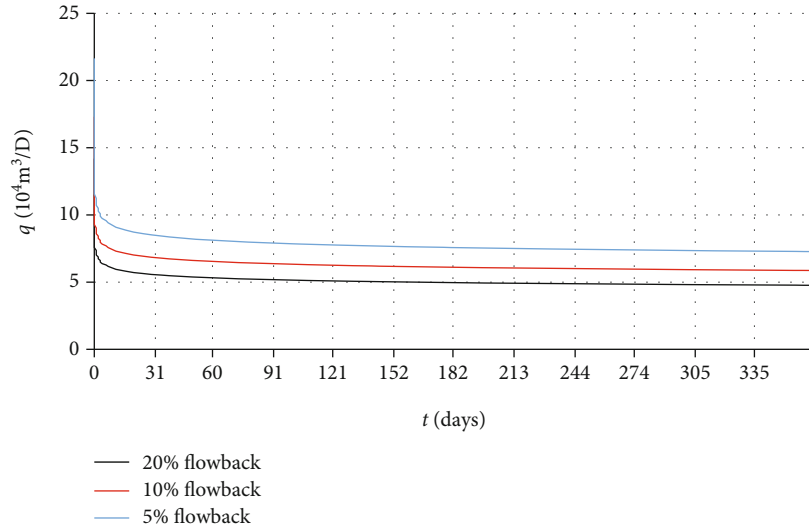


FIGURE 16: Change of gas production with time under different flowback rates after fracturing.

of fracturing fluid; (2) after that, the daily gas production decreased rapidly, and the influence of different liquid flowback rates on the daily gas production increased significantly; (3) after about 100 days, the daily gas production tends to be stable. When the production reaches one year, the daily gas production corresponding to the fracturing fluid flowback rate of 20%, 10%, and 5% is 47700 m^3 , 5800 m^3 , and 72700 m^3 , respectively. The calculation results prove the conclusion that less fracturing fluid flowback will produce more gas.

5. Summary and Conclusions

In this paper, the instantaneous source function and Newman product method are employed to obtain the formation pressure distribution during multistage fracturing of horizontal wells. It is taken as the initial pressure-distribution condition of gas-liquid two-phase numerical simulation, and the double pressure funnels and gas-liquid two-way mass transfer are investigated in detail. The main conclusions in this work are summarized as follows:

- (1) Double pressure funnels phenomenon exists during fracturing fluid flowback. After fracturing of shale gas well, a large amount of fracturing fluid accumulates near the fracture, forming a high-pressure area far higher than the original formation pressure, and a funnel is formed between the high-pressure area and the original formation pressure. During production stage, another pressure funnel is formed near the fracture. Eventually, there appear double pressure funnels around each fracture
- (2) Gas-liquid two-way mass transfer phenomenon exists between free gas and fracturing fluid. The funnel formed by the high-pressure area and the original formation pressure makes the liquid flow into the formation through seepage. At the same time, the gas concentration of fracturing fluid is far lower than that in the formation. Therefore, the gas diffuses from the

formation to the vicinity of the fracture through diffusion, forming gas-liquid two-way mass transfer

- (3) Double pressure funnels and gas-liquid two-way mass transfer explain the production phenomenon of “less fracturing fluid flowback but high-gas production.” Two conditions for the reasonable well shut-in time are also given, and they are the moving speed of the pressure boundary line should be less than 0.1 m/d , and the water-gas ratio near the fracture should be less than $(1/d)$ with time
- (4) It is found from PEBI grid numerical simulation that, when shale gas well is shut-in for 20 days and produce for 1 year, the daily gas production corresponding to fracturing fluid flowback rates of 20%, 10%, and 5% is 47700 m^3 , 5800 m^3 , and 72700 m^3 , respectively. The simulation results prove the production phenomenon of less fracturing fluid flowback but high-gas production
- (5) The fracturing fluid injected during fracturing leads to the formation of a high-pressure zone near the well, which is equivalent to supplementing the formation with a certain amount of energy, thus increasing the formation pressure during drainage. If the initial production of flowback is too large, the bottom-hole pressure will drop quickly and the production pressure difference will be large, which may lead to risks such as sand production and fracture closure. According to the double pressure funnels study, reasonable production can be determined to optimize shale gas production

The advantage of the study is as follows: using PEBI grid to realize exact characterize of fracture, and the analytical solution of pressure distribution after fracturing is used for numerical simulation of well shut-in and drainage process. The double pressure funnels and gas-liquid two-way mass transfer theory is put forward, some phenomena in shale gas development

are well explained, and the theory basis of reasonable well shut-in time and drainage optimization is provided.

For further research of the theory and application, the disadvantage and limitation of recent study are as follows:

Disadvantage. If free gas content in formation is too low, the accuracy of the method is relatively low.

Limit. For the calculation, rectangle reservoir model is applied, but for other shape models, the method needs to improve.

Abbreviations

k :	Formation permeability, μm^2
ϕ :	Formation porosity, dimensionless
h :	Effective thickness of the formation, m
μ :	Fluid viscosity of the formation, MPa·s
C_t :	Comprehensive compression coefficient, MPa^{-1}
$\chi = k/(\phi\mu C_t)$:	Coefficient of pressure conductivity, m^2/s
p_i :	Original formation pressure, MPa
x_f :	Half-length of the fracture, m
G :	Total amount of fracturing fluid injected, m^3
x_w :	Well location of axis x
y_w :	Well location of axis y
x_e :	Rectangular boundary of axis x
y_e :	Rectangular boundary of axis y
G_{ij} :	Geometric factor of two adjacent grids i and j , dimensionless
$T_{ij,l} = \lambda_{ij,l} G_{ij}$:	Conductivity coefficient of two adjacent grids i and j , $\text{m}^3/\text{Pa}\cdot\text{s}$
ω_{ij} :	The adjacent surface of two adjacent grids i and j , m^2
d_{ij} :	The distance of two adjacent grids, m
Z :	Height calculated from a certain datum, m
l :	Water and gas phase, dimensionless
k_{rl} :	Relative permeability of the l phase, dimensionless
μ_l :	Viscosity of the l phase, Pa·s
S_w :	Water saturation, dimensionless
S_g :	Gas saturation, dimensionless
f :	Solution variables of p , S_w , and S_g
C_g :	Gas compression coefficient, Pa^{-1}
V_i :	Volume of the i^{th} grid unit, m^3
t^{n+1} :	$n + 1$ time step length, s
t^n :	n time step length, s
D_m :	Gas diffusion coefficient, m^2/s
$c = m/v$:	Gas concentration, kg/m^3
M :	Unit molar mass of the gas mixture, kg/kmol
$R = 8.314$:	Universal gas constant, $\text{kg}/(\text{kmol}\cdot\text{k})$
Z :	Deviation factor of real gas, dimensionless
T :	Temperature, k
ρ :	Density, kg/m^3
c_g :	Compression coefficient, MPa^{-1}
V_g :	Free gas content, m^3/T .

Data Availability

The data used to support the findings of this study are available from the corresponding author upon request.

Conflicts of Interest

The authors declare that there is no conflicts of interest regarding the publication of this paper.

Acknowledgments

This work is supported by Basic Theory and Key Technology of Shale Gas Exploration and Development under Grant No. XDB10030402.

References

- [1] M. Glade, J. Speirs, and S. Sorrell, "Unconventional gas - a review of regional and global resource estimates," *Energy*, vol. 55, pp. 571–584, 2013.
- [2] C. Zou, D. Dong, Y. Wang et al., "Shale gas in China: characteristics, challenges and prospects (II)," *Petroleum Exploration and Development*, vol. 43, no. 2, pp. 182–196, 2016.
- [3] X. Ma, X. Li, F. Liang et al., "Dominating factors on well productivity and development strategies optimization in Weiyuan shale gas play, Sichuan Basin, SW China," *Petroleum Exploration and Development*, vol. 47, no. 3, pp. 594–602, 2020.
- [4] W. Shen, X. Li, T. Ma, J. Cai, X. Lu, and S. Zhou, "High-pressure methane adsorption behavior on deep shales: experiments and modeling," *Physics of Fluids*, vol. 33, no. 6, article 063103, 2021.
- [5] L. Han, X. Li, W. Guo et al., "Characteristics and dominant factors for natural fractures in deep shale gas reservoirs: a case study of the Wufeng-Longmaxi formations in Luzhou block, southern China," *Lithosphere*, vol. 2022, no. 1, article 9662175, 2022.
- [6] Y. Li, "Study of well shut-in technology after fracturing of horizontal well," *Liaoning Chemical Industry*, vol. 49, pp. 794–796, 2020.
- [7] A. Ibrahim and H. Nasr-El-Din, "Effect of well shut-in after fracturing operations on near wellbore permeability," *Journal of Petroleum Science and Engineering*, vol. 181, article 106213, 2019.
- [8] B. Lecampion, A. Bungler, and X. Zhang, "Numerical methods for hydraulic fracture propagation: a review of recent trends," *Journal of Natural Gas Science and Engineering*, vol. 49, pp. 66–83, 2018.
- [9] R. Lemoine and J. Lee, "Analytical scaling enhances production analysis of multi-fractured horizontal wells," in *SPE Western Regional Meeting*, San Jose, California, USA, 2019.
- [10] J. D. Williams-Kovacs and C. R. Clarkson, "Analysis of multi-well and stage-by-stage flowback from multi-fractured horizontal wells," in *SPE/CSUR Unconventional Resources Conference-Canada*, Calgary, Alberta, Canada, 2014.
- [11] L. Yang, C. Ping, and M. T. Shou, "Application of well factory drilling technology in shale gas development in the Sichuan basin," in *SPE/IATMI Asia Pacific Oil & Gas Conference and Exhibition*, Jakarta, Indonesia, 2017.
- [12] Y. Liu, D. Gao, Q. Li et al., "Mechanical frontiers in shale-gas development," *Advances in Mechanics*, vol. 49, article 201901, 2019.
- [13] Y. Hu, X. Li, Y. Wan et al., "Physical simulation on gas percolation in tight sandstones," *Petroleum Exploration and Development*, vol. 40, no. 5, pp. 621–626, 2013.

- [14] J. Ma, J. P. Sanchez, K. Wu, G. D. Couples, and Z. Jiang, "A pore network model for simulating non-ideal gas flow in micro- and nano- porous materials," *Fuel*, vol. 116, pp. 498–508, 2014.
- [15] J. Adachi, E. Siebrits, A. Peirce, and J. Desroches, "Computer simulation of hydraulic fractures," *International Journal of Rock Mechanics and Mining Sciences*, vol. 44, no. 5, pp. 739–757, 2007.
- [16] F. Civan, "Effective correlation of apparent gas permeability in tight porous media," *Transport in Porous Media*, vol. 82, no. 2, pp. 375–384, 2010.
- [17] C. Niu, Y. Z. Hao, D. Li, and D. Lu, "Second-order gas-permeability correlation of shale during slip flow," *SPE Journal*, vol. 19, no. 5, pp. 786–792, 2014.
- [18] O. Kresse, C. Cohen, X. Weng, R. Wu, and H. Gu, "Numerical modeling of hydraulic fracturing in naturally fractured formations," in *45th U.S. Rock Mechanics/Geomechanics Symposium*, San Francisco, California, 2011.
- [19] A. Settari and M. P. Cleary, "Three-dimensional simulation of hydraulic fracturing," *Journal of Petroleum Technology*, vol. 36, no. 7, pp. 1177–1190, 1984.
- [20] M. Chen, S. Zhang, Y. Xu, X. Ma, and Y. Zou, "A numerical method for simulating planar 3D multi-fracture propagation in multi-stage fracturing of horizontal wells," *Petroleum Exploration and Development*, vol. 47, no. 1, pp. 171–183, 2020.
- [21] E. V. Dontsov and A. P. Peirce, "A non-singular integral equation formulation to analyse multiscale behaviour in semi-infinite hydraulic fractures," *Journal of Fluid Mechanics*, vol. 781, pp. 248–254, 2015.
- [22] J. Wen, W. Tian, Q. Bi, X. Li, and D. Lu, "A new data inversion analysis method based on digital filtered pump-stop data of hydraulic fracturing," *Journal of University of Science and Technology of China*, vol. 48, pp. 392–399, 2018.
- [23] W. Yu, K. Wu, L. Zuo, J. Miao, and K. Sepehrnoori, "Embedded discrete fracture model assisted study of gas transport mechanisms and drainage area for fractured shale gas reservoirs," in *SPE/AAPG/SEG Unconventional Resources Technology Conference*, Denver, Colorado, USA, 2019.
- [24] Y. Chen, Z. Qu, Y. Ding, T. Guo, Y. Bai, and J. Wang, "Unified backflow model after multilayer hydraulic fracturing," *Fault-Block Oil&Gas Field*, vol. 27, pp. 484–488, 2020.
- [25] E. Eltahan, F. Bordeaux Rego, W. Yu, and K. Sepehrnoori, "Impact of well shut-in after hydraulic-fracture treatments on productivity and recovery in shale oil reservoirs," in *SPE Improved Oil Recovery Conference*, 2020.
- [26] N. Wijaya and J. Sheng, "Effects of imbibition and compaction during well shut-in on ultimate shale oil recovery: a numerical study," *SPE Reservoir Evaluation & Engineering*, vol. 24, no. 4, pp. 859–873, 2021.
- [27] L. Tao, J. Guo, Y. Lu et al., "Experimental study on shut-in-time optimization for multi-fractured horizontal wells in shale reservoirs," in *SPE International Hydraulic Fracturing Technology Conference & Exhibition*, Muscat, Oman, 2022.
- [28] Y. Wu, L. Cheng, L. Ma et al., "A transient two-phase flow model for production prediction of tight gas wells with fracturing fluid-induced formation damage," *Journal of Petroleum Science and Engineering*, vol. 199, article 108351, 2021.
- [29] D. Lu, *Modern Well Testing Theory and Application*, Petroleum Industry Press (in Chinese), Beijing, 2009.
- [30] X. Kong, *Advanced Mechanics of Fluids in Porous Media*, Press of University of Science and Technology of China (in Chinese), Hefei, 3rd edition, 2020.
- [31] H. Deng, X. Bao, Z. Chen, and R. Wang, "Numerical Well Testing Using Unstructured PEBI Grids," in *SPE Middle East Unconventional Gas Conference and Exhibition*, Muscat, Oman, 2011.
- [32] D. Li and W. Zha, *Numerical Well Testing: Theory and Method*, Petroleum Industry Press (in Chinese), Beijing, 2013.
- [33] G. Karimi, X. Li, and P. Teertstra, "Measurement of through-plane effective thermal conductivity and contact resistance in PEM fuel cell diffusion media," *Electrochimica Acta*, vol. 55, no. 5, pp. 1619–1625, 2010.
- [34] F. Zhang and H. Emami-Meybodi, "Flowback fracture closure of multi-fractured horizontal wells in shale gas reservoirs," *Journal of Petroleum Science and Engineering*, vol. 186, article 106711, 2020.
- [35] Y. Cai and A. Dahi Taleghani, "Pursuing improved flowback recovery after hydraulic fracturing," in *SPE Eastern Regional Meeting*, Charleston, West Virginia, USA, 2019.
- [36] X. Li, D. Lu, R. Luo, Y. Sun, and W. Shen, "Quantitative criteria for identifying main flow channels in complex porous media," *Petroleum Exploration and Development*, vol. 46, no. 5, pp. 998–1005, 2019.